

Neutrino decay confronts the SNO data

Abhijit Bandyopadhyay^{a*}, Sandhya Choubey^{b†}, Srubabati Goswami^{a‡}

^a*Theory Group, Saha Institute of Nuclear Physics,
1/AF, Bidhannagar, Calcutta 700 064, INDIA*

^b*Department of Physics and Astronomy, University of Southampton,
Highfield, Southampton S017 1BJ, UK*

February 8, 2020

Abstract

We investigate the status of the neutrino decay solution to the solar neutrino problem in the context of the recent results from Sudbury Neutrino Observatory (SNO). We present the results of global χ^2 -analysis for both two and three generation cases with one of the mass states being allowed to decay and include the effect of both decay and mixing. We find that the Large Mixing Angle (LMA) region which is the currently favoured solution of the solar neutrino problem is affected significantly by decay. We obtain bounds on the decay constant α in this region which implies a rest frame life time $\tau_0/m > 1.5 \times 10^{-5}$ sec/eV for the unstable neutrino state. We present the allowed areas in the $\Delta m^2 - \tan^2 \theta$ plane for different allowed values of α and examine how these areas change with the inclusion of decay. Finally we show that the forthcoming neutral current data from SNO can further constrain the allowed values of α , Δm^2 and $\tan^2 \theta$.

*e-mail: abhi@theory.saha.ernet.in

†email: sandhya@hep.phys.soton.ac.uk

‡e-mail: sruba@theory.saha.ernet.in

1 Introduction

The comparison of the recent SNO charged current (CC) measurements with the neutrino electron scattering rate observed in SuperKamiokande (SK) has established the presence of ν_μ and/or ν_τ component in the solar neutrino flux at more than 3σ level [1]. It is pertinent to ask at this point whether conversions to sterile neutrinos are allowed or not. One of the scenarios in which one can have a final sterile state is neutrino decay. The aim of this paper is to investigate the status of the neutrino decay solution to the solar neutrino problem with the incorporation of the SNO data. We deal with both two generation and three generation cases. For the latter we consider three flavor mixing between ν_e , ν_μ and ν_τ with mass eigenstates ν_1 , ν_2 and ν_3 with the assumed mass hierarchy as $m_1^2 < m_2^2 < m_3^2$. The lightest neutrino mass state is assumed to have lifetime much greater than the sun-earth transit time and hence can be taken as stable. Whereas the heavier mass states ν_2 and ν_3 may be unstable. But the CHOOZ data [2] constrains the mixing matrix element U_{e3} to a very small value which implies very small mixture of the ν_3 state to the ν_e state produced in sun. So the instability of the ν_3 state has hardly any effect on solar neutrino survival probability, and to study the effect of decay on solar neutrinos for simplicity we can consider only the second mass state ν_2 to be unstable.

There are two kinds of models of non-radiative decays of neutrinos

- If neutrinos are Dirac particles one has the decay channel $\nu_2 \rightarrow \bar{\nu}_{1R} + \phi$, where $\bar{\nu}_{1R}$ is a right handed singlet and ϕ is an iso-singlet scalar [3]. Thus all the final state particles are sterile.
- If neutrinos are Majorana particles, the decay mode is $\nu_2 \rightarrow \bar{\nu}_1 + J$, where $\bar{\nu}_1$ interacts as a $\bar{\nu}_e$ with a probability $|U_{e1}|^2$ and J is a Majoron [4].

In both scenarios the rest frame lifetime of ν_2 is given by [5]

$$\tau_0 = \frac{16\pi m_2(1 + m_1/m_2)^{-2}}{g^2 \Delta m^2} \quad (1)$$

where g is the coupling constant and $\Delta m^2 (= m_2^2 - m_1^2)$ is the mass squared difference between the states involved in the decay process. If a neutrino of energy E decays while traversing a distance L then the decay term $\exp(-\alpha L/E)$ gives the fraction of neutrinos that decay. α is the decay constant and is related to τ_0 as $\alpha = m_2/\tau_0$.

For the sun-earth distance of 1.5×10^{11} m, and for a typical neutrino energy of 10 MeV one starts getting appreciable decay for $\alpha \sim 10^{-12}$ eV². For lower values of α the $\exp(-\alpha L/E)$ term goes to 1 signifying no decay while for $\alpha > 10^{-10}$ eV² the exponential term goes to zero signifying complete decay of the unstable neutrinos. Assuming $m_2 \gg m_1$ the equation (1) can be written as

$$g^2 \Delta m^2 \sim 16\pi\alpha \quad (2)$$

If we now incorporate the bound $g^2 < 4.5 \times 10^{-5}$ as obtained from K decay modes [6] we get the bound $\Delta m^2 > 10^6\alpha$. This gives the range $\Delta m^2 \gtrsim 10^{-6}$ eV² for which we can have appreciable decay. Neutrino decay in the context of the solar neutrino problem has been considered earlier in [3, 4, 7] and more recently in [8, 9, 10]. After the declaration of the SNO CC data, bounds on

the decay constant α has been obtained from the data on total rates [11] as well as from SK and SNO spectrum data [12]. In this paper we do a combined global statistical analysis of the solar neutrino data including the total rates from the Cl, Ga, SK and SNO CC experiments as well as the electron recoil energy spectrum from SK [1, 13]. We do our analysis for both two and three generation scenarios. We include the results of the CHOOZ experiment [2] in our three generation analysis. In section 2 we briefly present the survival probability for the solar neutrinos with one of the components unstable. In section 3 we first find the constraints coming from inclusion of the SNO CC data within a two-generation framework. We next extend our analysis to include the third neutrino flavor and present bounds on α , Δm_{21}^2 and $\tan^2 \theta_{21}$ for different allowed values of θ_{13} , from a χ^2 analysis which includes both the global solar neutrino data as well as the CHOOZ data. We explore the potential of the SNO neutral current data (NC) in constraining the decay and oscillation parameters in section 4. We end with conclusions in section 5.

2 Formalism

The three-generation mixing matrix relating the mass and flavour eigenstates are given as

$$\begin{aligned}
 U &= R_{23}R_{13}R_{12} \\
 &= \begin{pmatrix} c_{13}c_{12} & s_{12}c_{13} & s_{13} \\ -s_{12}c_{23} - s_{23}s_{13}c_{12} & c_{23}c_{12} - s_{23}s_{13}s_{12} & s_{23}c_{13} \\ s_{23}s_{12} - s_{13}c_{23}c_{12} & -s_{23}c_{12} - s_{13}s_{12}c_{23} & c_{23}c_{13} \end{pmatrix} \quad (3)
 \end{aligned}$$

where we neglect the CP violation phases.

Allowing for the possibility of decay of the second mass eigenstate the probability of getting a neutrino of flavour f starting from an initial electron neutrino flavour is ¹.

$$\begin{aligned}
 P_{ef} &= a_{e1}^{\odot 2} |A_{1f}^{\oplus}|^2 + a_{e2}^{\odot 2} |A_{2f}|^2 e^{-\alpha(L-R_{\odot})/E} + a_{e3}^{\odot 2} |A_{3f}^{\oplus}|^2 \\
 &+ 2a_{e1}^{\odot} a_{e2}^{\odot} e^{-\alpha(L-R_{\odot})/2E} \text{Re}[A_{1f}^{\oplus} A_{2f}^{\oplus*} e^{i(E_2-E_1)(L-R_{\odot})} e^{i(\phi_{2,\odot}-\phi_{1,\odot})}] \quad (4)
 \end{aligned}$$

where E_i is the energy of the mass eigenstate i , E is the energy of the neutrino beam, α is the decay constant, L is the distance from the center of the sun, R_{\odot} is the radius of the sun, $\phi_{i,\odot}$ are the phase inside the sun and a_{ei}^{\odot} is the amplitude of an electron state to be in the mass eigenstate ν_i at the surface of the sun [15]

$$a_{ei}^{\odot 2} = \sum_{j=1,2,3} X_{ij} U_{je}^{\odot 2} \quad (5)$$

where X_{ij} denotes the non-adiabatic jump probability between the i^{th} and j^{th} states inside the sun and U_{je}^{\odot} denotes the mixing matrix element between the flavour state ν_e and the mass eigenstate ν_j in sun. A_{if}^{\oplus} denote the $\nu_i \rightarrow \nu_f$ transition amplitudes inside the earth. We evaluate these amplitudes numerically by assuming the earth to consist of two constant density slabs [15]. It can be shown that the square bracketed term containing the phases averages out to zero in the range of Δm^2 in which we are interested [16]. For further details of the calculation of the survival probability we refer to [15].

¹For a rigorous derivation of the probability for the decay plus oscillation scenario see [14].

In the two generation limit the ν_e survival probability including earth matter effects and decay can be expressed as [9]

$$P_{ee} = P_{ee}^{\text{day}} + \frac{(\sin^2 \theta - P_{2e})(P_{ee}^{\text{day}} + e^{-2\alpha(L-R_\odot)/E}(P_{ee}^{\text{day}} - 1))}{\cos^2 \theta - \sin^2 \theta e^{-2\alpha(L-R_\odot)/E}} \quad (6)$$

where P_{2e} is the transition probability of $\nu_2 \rightarrow \nu_e$ at the detector while P_{ee}^{day} is the day-time survival probability (without earth matter effects) for ν_e and is given by [9]

$$P_{ee}^{\text{day}} = \cos^2 \theta [P_J \sin^2 \theta_M + (1 - P_J) \cos^2 \theta_M] + \sin^2 \theta [(1 - P_J) \sin^2 \theta_M + \cos^2 \theta_M P_J] e^{-2\alpha(L-R_\odot)/E_2} \quad (7)$$

where P_J is the non-adiabatic level jumping probability between the two mass eigenstates for which we use the standard expression from [17] and θ_M is the matter mixing angle given by

$$\tan 2\theta_M = \frac{\Delta m^2 \sin 2\theta}{\Delta m^2 \cos 2\theta - 2\sqrt{2}G_F n_e E}. \quad (8)$$

n_e being the ambient electron density, E the neutrino energy, and $\Delta m^2 (= m_2^2 - m_1^2)$ the mass squared difference in vacuum.

From eq.(7) we note that the decay term appears with a $\sin^2 \theta$ and is therefore appreciable only for large enough θ . Thus we expect the effect of decay to be maximum in the LMA region. This can also be understood as follows. The ν_e are produced mostly as ν_2 in the solar core. In the LMA region the neutrinos move adiabatically through the sun and emerge as ν_2 which eventually decays. For the SMA region on the other hand P_J is non-zero and ν_e produced as ν_2 cross over to ν_1 at the resonance and come out as a ν_1 from the solar surface. Since ν_1 is stable, decay does not affect this region.

3 Analysis of data and results

3.1 Bounds from two-generation analysis

First we use the standard χ^2 minimisation procedure and determine the goodness of fit (GOF) and the best-fit values of the oscillation and decay parameters, in a two flavor mixing scenario. Details of our statistical analysis procedure, including the definition of the χ^2 and the correlated error matrix are given in [9, 18, 19, 20], while the experimental data used has been summarised in [19, 20]. We incorporate the total rate in Cl, Ga and SK and the SNO CC rate along with the SK spectrum data. We find that the global best-fit comes in the LMA region with the decay constant $\alpha = 0$ and $\tan^2 \theta = 0.37$, $\Delta m^2 = 4.63 \times 10^{-5} \text{eV}^2$, the 8B flux being kept fixed at the SSM value².

²The bounds that we give here and subsequently apply to the decay model where both final states are sterile. In the Majoron decay model the final state $\bar{\nu}_e$ can interact in the SK/SNO detectors although with an energy degradation. In [9] we have shown that if we use the bound on the $\bar{\nu}_e$ flux from SK, then such models are constrained more severely. An interesting possibility where the absolute mass scales of the two neutrino states are approximately degenerate and hence the daughter $\bar{\nu}_e$ is not degraded in energy is considered recently in [12].

In figure 1 we plot for two-generations the $\Delta\chi^2$ ($=\chi^2 - \chi_{min}^2$) for the neutrino decay scenario, against the decay constant α , keeping Δm^2 and $\tan^2\theta$ free. The figure shows that the fit becomes worse with increasing value of the decay constant. We remind the reader that neutrino decay is important only for LMA and for each value of α on this curve the minimum χ^2 comes with Δm^2 and $\tan^2\theta$ in the LMA region. Its known that the inclusion of the SNO data in the global solar neutrino analysis improves the fit in the LMA region for stable neutrinos [20, 21]. Hence for small values of α where neutrinos can be taken as almost stable, the inclusion of the SNO data gives a better GOF. However as α increases the neutrino decay leads to more sterile components in the final state – which is disfavoured by the SNO/SK combination and the GOF worsens with SNO included. As is seen from figure 1, inclusion of the SNO CC rate puts an upper bound on the decay constant – $\alpha < 4.3 \times 10^{-11} \text{eV}^2$ at 99% C.L., when Δm^2 and θ are allowed to take on any value.

In figure 2 we plot the allowed areas in the Δm^2 - $\tan^2\theta$ plane for different allowed values of the decay constant α for a two flavor scenario and with global data including SNO CC rate. The figure shows that the allowed area in the LMA region is reduced as α increases. As α increases the spectral distortion increases and the effect is more for higher(lower) values of $\tan^2\theta$ (Δm^2) [9]. For this reason these regions get disallowed with increasing α . For the high Δm^2 regions the spectral distortion does not increase significantly with increasing α . However the low energy neutrinos relevant for *Ga* experiment decay more making the fit to the total rates worse. Therefore even the high Δm^2 regions get more and more disfavored with increasing α .

As discussed earlier, for small values of mixing angles the fraction of the decaying component in the ν_e beam ($\sim \sin^2\theta$) being very small decay does not have much effect. Hence no new feature is introduced in the SMA region because of decay and it remains disallowed at 3σ level by the global data. On the other hand, in the LOW region though mixing is large, due to small Δm^2 any appreciable decay over the sun-earth distance is not obtained, if the bound on the coupling constant from K-decay [6] is to be accounted for. Therefore, LOW region in the parameter space remains unaffected by the unstable ν_2 state, and we do not show it explicitly in figure 2.

3.2 Bounds from three-generation analysis

Next we investigate the impact of the unstable ν_2 mass state on the three flavor oscillation scenario with $\Delta m_{21}^2 = \Delta m_{\odot}^2$ and $\Delta m_{31}^2 = \Delta m_{CHOOZ}^2 \simeq \Delta m_{atm}^2 = \Delta m_{32}^2$. For the three generation case the χ^2 is defined as

$$\chi^2 = \chi_{solar}^2 + \chi_{chooz}^2 \quad (9)$$

For the expressions of χ_{solar}^2 and χ_{chooz}^2 we refer the reader to [15]. In figure 3 we plot the $\Delta\chi^2$ ($=\chi^2 - \chi_{min}^2$) vs α for various fixed values of θ_{13} allowing the other parameters to take arbitrary values. Δm_{31}^2 is varied within the allowed range $[1.5 - 6.0] \times 10^{-3} \text{eV}^2$ as obtained from a combined analysis of atmospheric and CHOOZ data [22, 23]. This figure indicates the allowed range of α for a fixed θ_{13} . As θ_{13} increases the contribution from χ_{chooz}^2 increases shifting the plots upwards. Consequently the curve corresponding to higher $\tan^2\theta_{13}$ crosses the 99% C.L. limit at a lower α and a more stringent bound is obtained as compared to smaller $\tan^2\theta_{13}$ cases. This figure also shows that for the three generation case the $\tan^2\theta_{13} = 0$ limit allows all values of α as opposed

to the two generation case. However that does not mean a better GOF for the three generation solution. This is reflected in figure 4 where we plot the GOF vs. α for the two generation case as well as the three generation case with $\tan^2 \theta_{13} = 0$.

In figure 5 we plot the allowed areas in the $\tan^2 \theta_{12}-\Delta m_{21}^2$ plane for different sets of values of $\tan^2 \theta_{13}$ and Δm_{31}^2 at different values of α . For fixed values of $\tan^2 \theta_{13}$ and Δm_{31}^2 the allowed area decreases with increasing α because of increased spectral distortion. At any given α the allowed area shrinks with the increase of $\tan^2 \theta_{13}$ and Δm_{31}^2 . This is again an effect of the CHOOZ data.

4 What can the SNO NC data tell us ?

The NC data from the SNO experiment is to be declared soon. In this section we discuss the effect of including the NC data in our χ^2 analysis. The combination of the SNO CC and SK elastic scattering rates predicts a NC rate of 1.0 ± 0.24 . The uncertainty is large because the SK elastic scattering rate has a lower sensitivity (by a factor of $\approx \frac{1}{6} - \frac{1}{7}$) to the ν_μ/ν_τ induced events. The NC data is expected to have a lower uncertainty – $\pm 8\%$ i.e. same as the CC rate and will eventually go down to 5%. In this work we assume the more conservative estimate and use $R_{NC} = 0.8 \pm 0.08, 1.0 \pm 0.08$ and 1.2 ± 0.08 as three representative values of the expected SNO NC rate [24] and examine if it can further constrain the neutrino decay scenario. For neutrino decay

$$R_{SNO}^{NC} = f_B(P_{ee} + P_{e\mu} + P_{e\tau}) \quad (10)$$

where f_B is the 8B flux normalisation factor. For this case the quantity in the paranthesis ($P_{ee} + P_{e\mu} + P_{e\tau}$) $\neq 1$ and the NC data does not directly give the 8B normalisation. Nevertheless it has a strong correlation with the 8B flux normalisation factor f_B . Therefore we keep f_B as a free parameter in our analysis including the expected NC rate and switch off the SSM 8B uncertainty which is much higher ($\sim 20\%$). We then perform a global χ^2 analysis of the Cl+Ga+SK+SNO CC+SNO NC+SK spectral data in framework of two-generations and put bounds on the allowed values of the mass and mixing parameters and look for constraints on α .

Figure 6 shows the χ^2 vs α incorporating the three representative NC rates. We find that as the NC rate increases there is less room for a sterile component in the final state and one gets a stronger constraint on the decay constant α . In figure 7 we give the allowed areas in the $\Delta m^2 - \tan^2 \theta$ plane incorporating the three tentative NC rates in the χ^2 analysis. The inclusion of the NC data reduces the size of the allowed regions.

5 Conclusions

In this paper we have done a global χ^2 analysis of the solar neutrino data assuming neutrino decay. We incorporate the recent SNO results. We present results for both two and three generation scenarios. We find that the best fit is obtained in the LMA region with the decay constant α zero i.e. for the no decay case. However nonzero values of α remain allowed. For the two generation case the bound at 99% C.L. on α that one gets after including the SNO data is $\alpha \leq 4.3 \times 10^{-11} \text{eV}^2$. This corresponds to a rest frame lifetime $\tau_0/m_2 > 1.5 \times 10^{-5} \text{s/eV}$. This is consistent with astrophysics

and cosmology. The effect of decay is not important in the SMA region because the decaying fraction in the solar ν_e beam goes as $\sin^2 \theta$ and this region remains disallowed. There is no change in the allowed areas in the LOW region also because eq. 2 and the bounds on the coupling constant from K decays restricts $\Delta m^2 \gtrsim 10^{-6}$ eV² and decay does not take place in the LOW region. The three generation analysis gives stronger bounds on α for non-zero θ_{13} . We repeat our two-generation oscillation analysis including decay by introducing three representative values of the anticipated SNO NC rate. The inclusion of the SNO NC data can severely constrain the parameter space in presence of decay.

References

- [1] SNO Collaboration, Q.R. Ahmed ,*et al.*nucl-ex/0106015
- [2] M. Appolonio *et al.*, Phys. Lett. **B466**, 415 (1999); Phys. Lett. **B420**, 397 (1998).
- [3] A. Acker, S. Pakvasa and S. Pantaleone, Phys. Rev. **D43**, R1754 (1991); Phys. Rev. **D45**, R1 (1992).
- [4] A. Acker, S. Pakvasa and A. Joshipura , Phys. Lett. **B285**, 371 (1992).
- [5] A. Acker and S. Pakvasa, Phys. Lett. **B320**, 320 (1994).
- [6] V. Barger, W.Y.Keung and S. Pakvasa, Phys. Lett. **B192**, 460 (1987).
- [7] R.S. Ragahavan, X. He and S. Pakvasa, Phys. Rev. **D38**, 1317 (1988).
- [8] S. Choubey, S. Goswami and D. Majumdar, Phys. Lett. **B484**, 73 (2000).
- [9] A. Bandyopadhyay, S. Choubey and S. Goswami, Phys. Rev. **D63**, 113019 (2001).
- [10] Chih-Kang Chou and M. Cho, Phys. Scripta **64**, 197 (2001).
- [11] A.S. Joshipura, E. Masso and S. Mohanty, hep-ph/0203181.
- [12] J.F. Beacom and N.F. Bell, hep-ph/0204111.
- [13] Y. Suzuki *et al.*, Super-Kamiokande collaboration, Nucl. Phys. Proc. Suppl. **77**, 35 (1999); B. Cleveland *et al.*, Ap. J. **496**, 505 (1998);J. N. Abduratshitov et al., SAGE collaboration, Phys. Rev. **C 60**, 055801 (1999); W. Hampel *et al.*, GALLEX collaboration, Phys. Lett. **B447**, 127 (1999); M. Altman *et al.*, GNO collaboration, Phys. Lett. **B490**, 16 (2000); Q. Ahmed et al, SNO collaboration, nucl-ex/0106015.
- [14] M. Lindner, T. Ohlsson and W. Winter, Nucl. Phys. **B607**, 326, 2001.
- [15] A. Bandyopadhyay, S. Choubey, S. Goswami and K. Kar, eprint archive: hep-ph/0110307 (to appear in Phys. Rev **D**).

- [16] A.S. Dighe, Q.Y. Liu and A. Yu. Smirnov, eprint archive: hep-ph/9903329.
- [17] S.T. Petcov, Phys. Lett. **B200**, 373 (1988).
- [18] S. Goswami, D. Majumdar, A. Raychaudhuri, Phys. Rev. **D63**, 013003, 2001; S. Choubey, S. Goswami, N. Gupta and D.P. Roy, Phys. Rev. **D64**, 053002 (2001).
- [19] S. Choubey, S. Goswami, K. Kar, H.M. Antia and S.M. Chitre, Phys. Rev. **D64**, 113001 (2001); S. Choubey, S. Goswami and D.P. Roy, Phys. Rev. **D65**, 073001 (2002).
- [20] A. Bandyopadhyay, S. Choubey, S. Goswami and K. Kar, Phys. Lett. **B519**, 83 (2001).
- [21] G.L. Fogli, E. Lisi, D. Montanino, A. Palazzo, Phys. Rev. **D64**, 093007 (2001); J.N. Bahcall, M.C. Gonzalez-Garcia, C. Pena-Garay, JHEP **0108**, 014 (2001); P.I. Krastev and A.Yu. Smirnov, e-Print Archive: hep-ph/0108177; M.V. Garzelli and C. Giunti, JHEP **0112**, 017 (2001).
- [22] M.C. Gonzalez-Garcia, M. Maltoni, C. Pena-Garay and J.W.F. Valle, Phys. Rev. **D63**, 033005, (2001).
- [23] G.L. Fogli, E. Lisi, A. Montanino and A. Palazzo, hep-ph/0104221.
- [24] A. Bandyopadhyay, S. Choubey, S. Goswami and D.P. Roy, hep-ph/0203169.

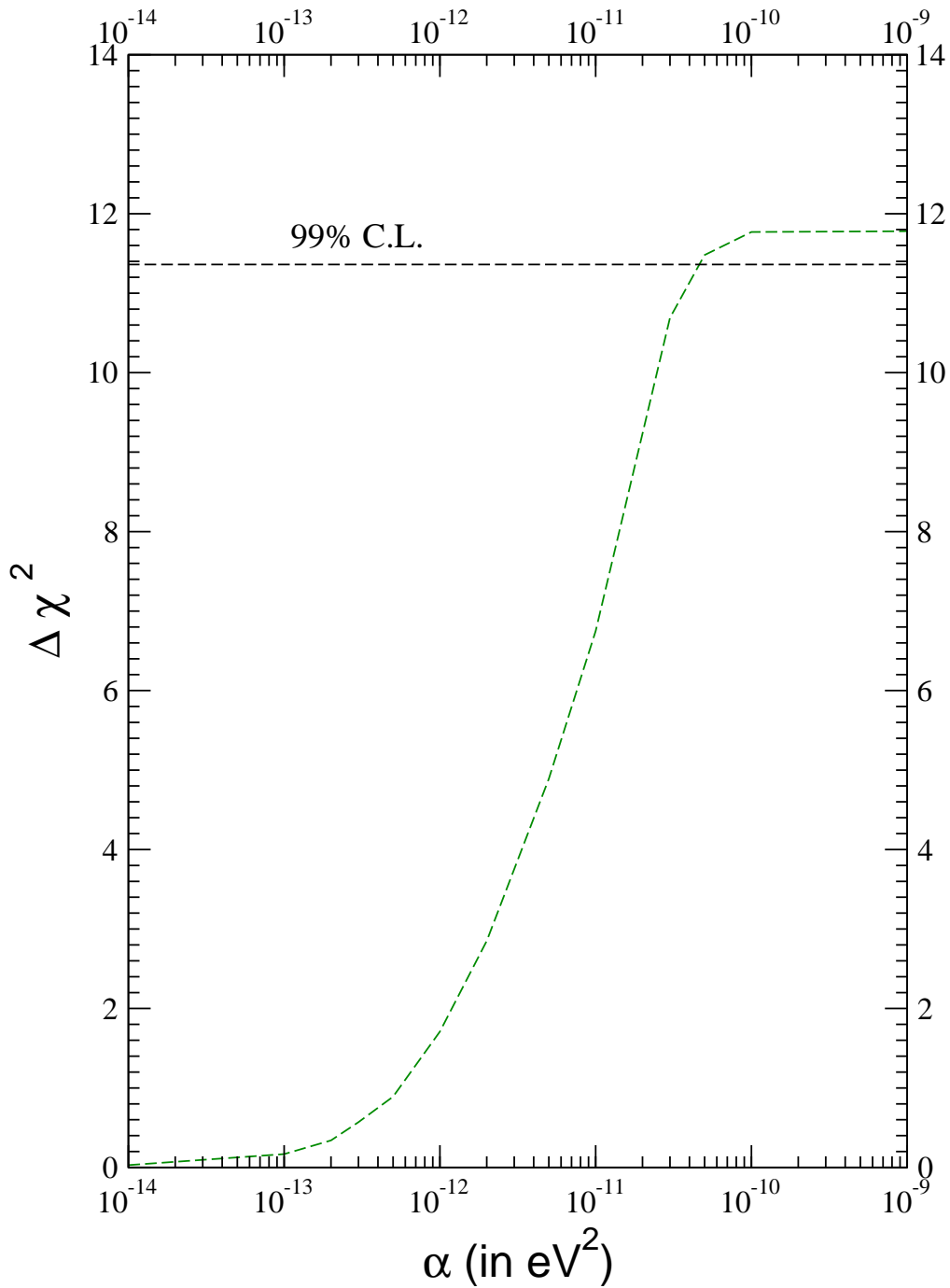


Figure 1: $\Delta\chi^2(= \chi^2 - \chi_{min}^2)$ vs decay constant α . Also shown is the 99% C.L. limit for three-parameters.

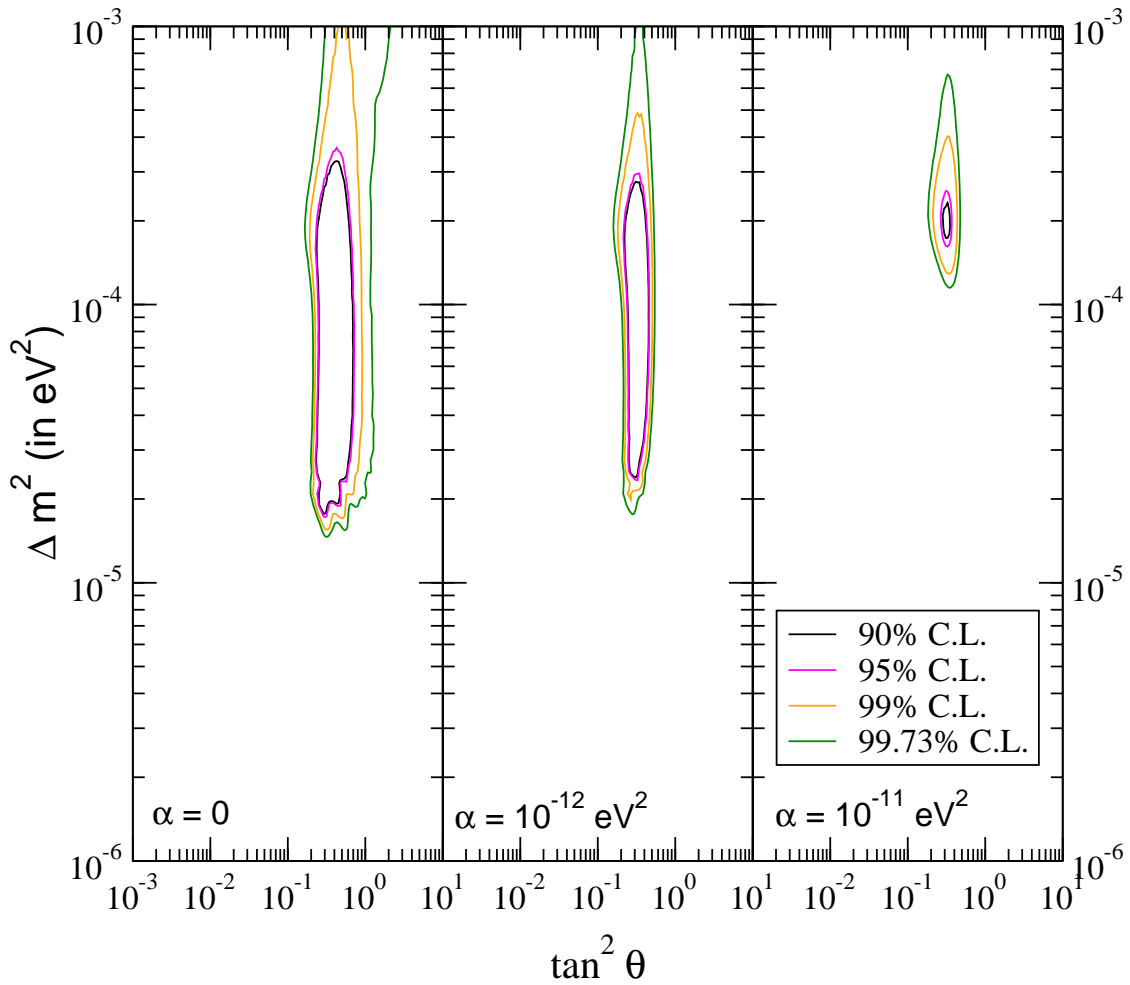


Figure 2: The 90, 95, 99 and 99.73% C.L. allowed area from the two-generation global analysis of the total rates and the SK recoil electron spectrum data in presence of decay and oscillation.

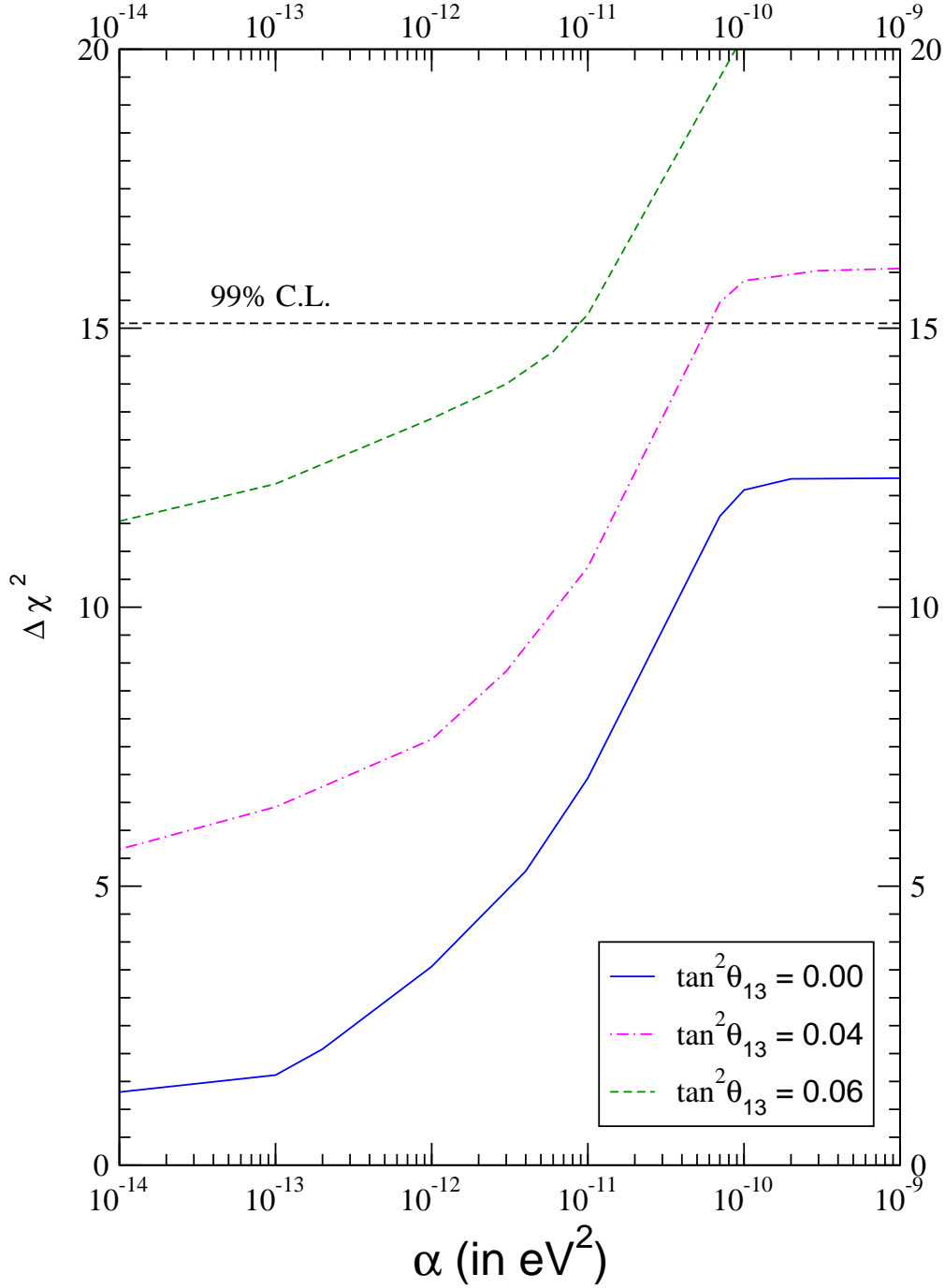


Figure 3: The $\Delta\chi^2(\chi^2 - \chi_{min}^2)$ vs decay constant α for the three generation case for various fixed values of θ_{13} with the other parameters allowed to vary freely.

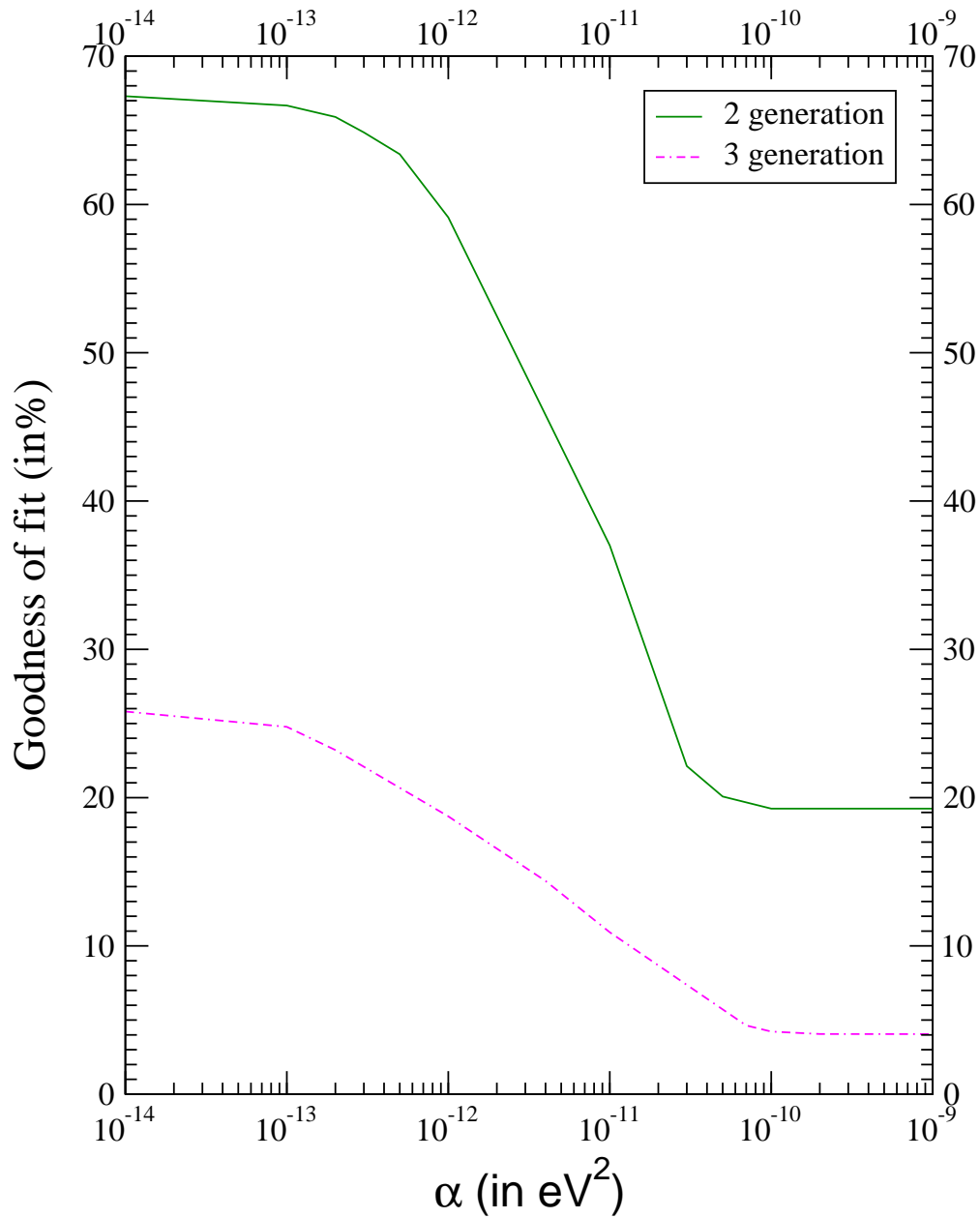


Figure 4: The GOF vs. α for the two generation case and the three generation case with $\tan^2 \theta_{13} = 0$.

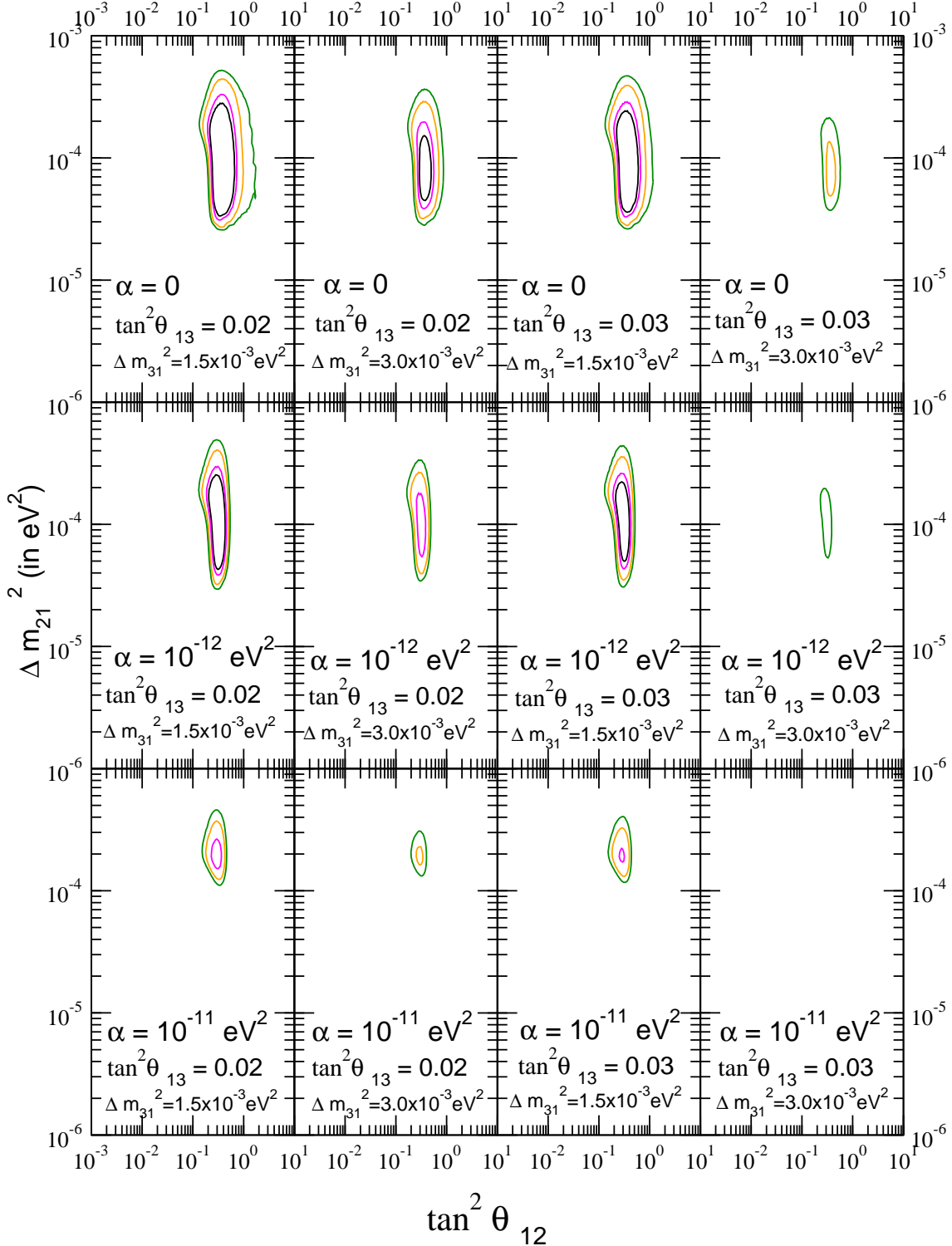


Figure 5: The 90, 95, 99 and 99.73% C.L. allowed area from the three-generation global analysis of the total rates and the SK recoil electron spectrum data in presence of decay and oscillation.

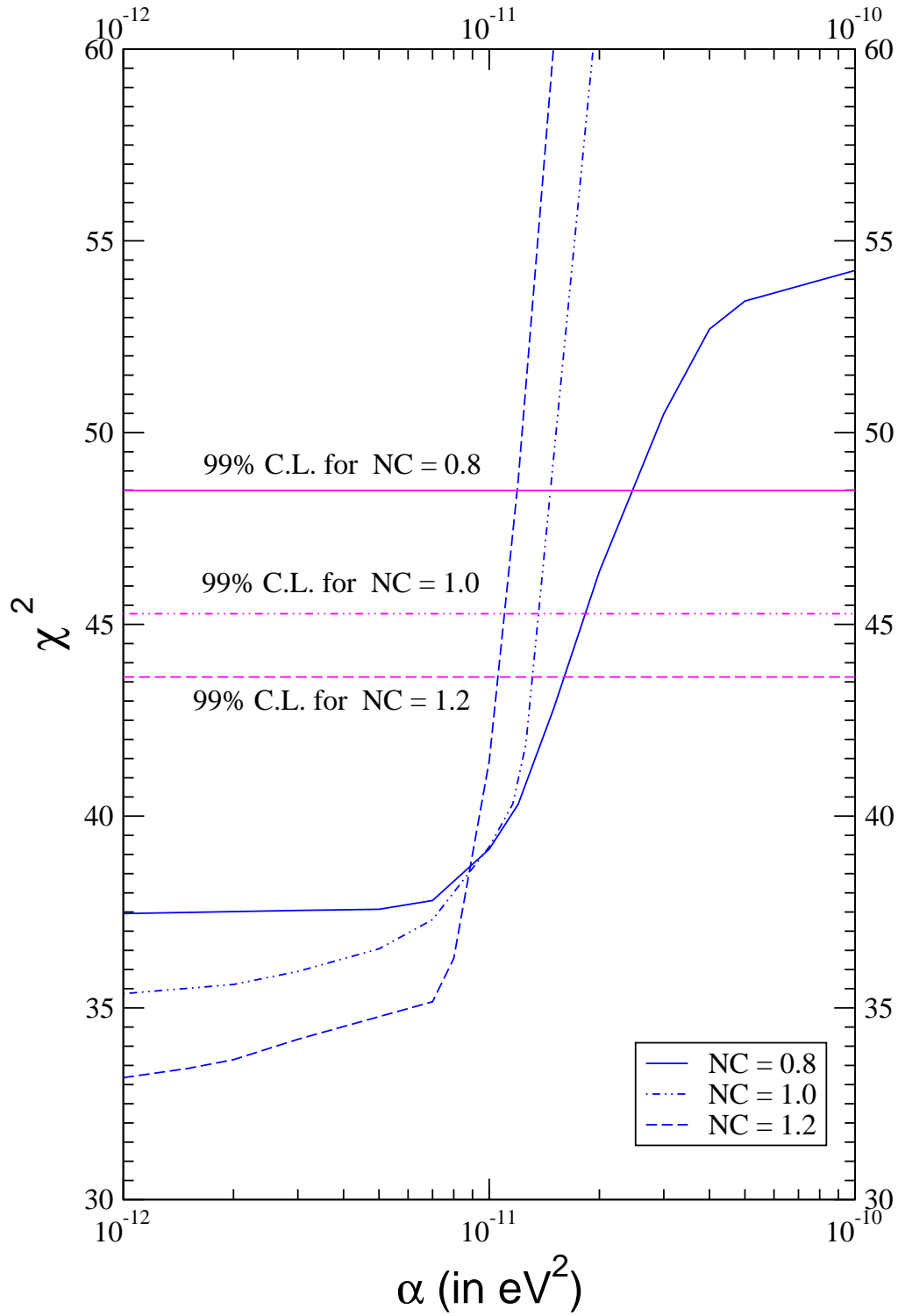


Figure 6: χ^2 vs decay constant α for three anticipated values of SNO NC rate.

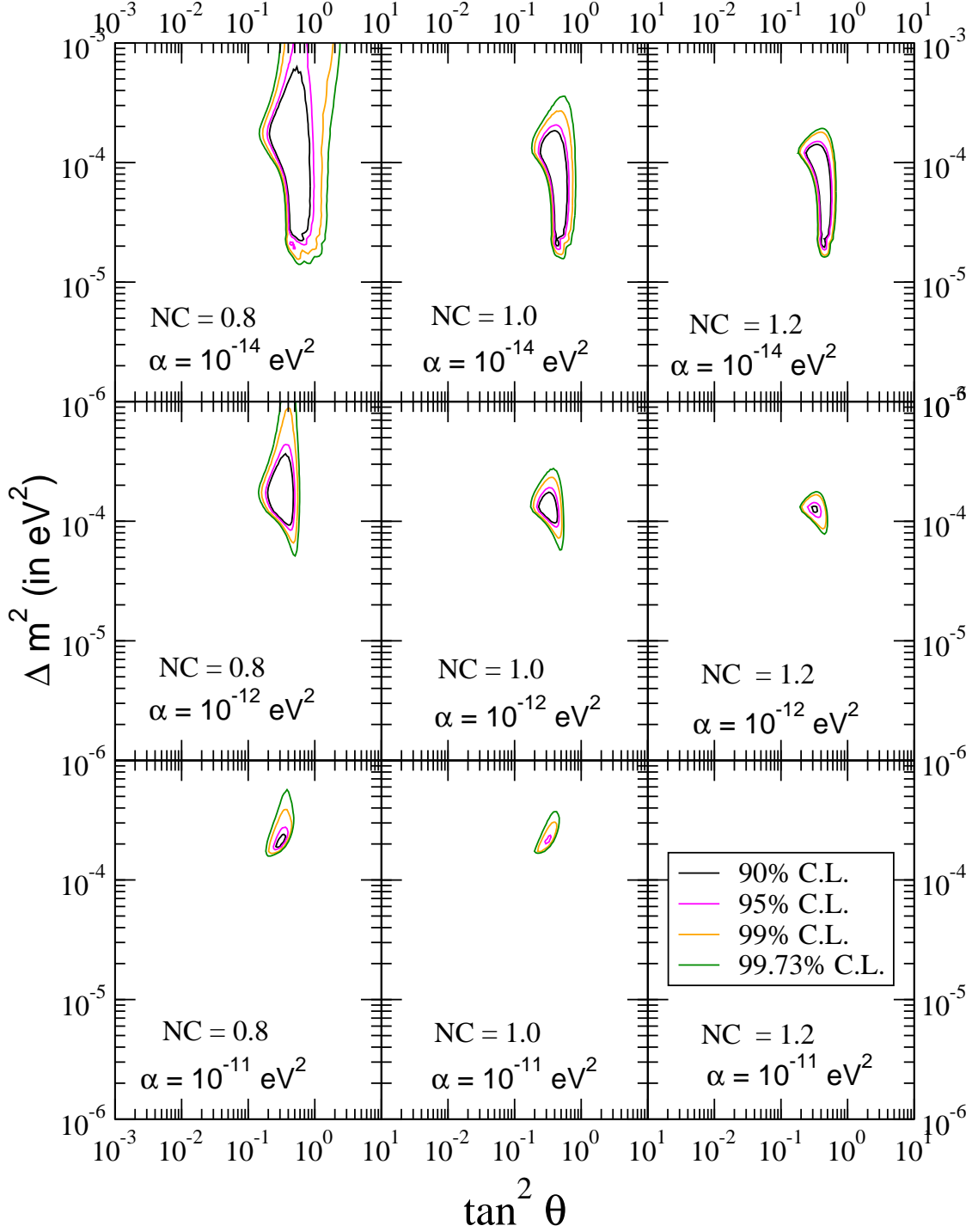


Figure 7: The 90, 95, 99 and 99.73% C.L. allowed area from the two-generation global analysis including the anticipated SNO NC rates and keeping the 8B flux normalisation factor f_B as a free parameter.